

Article

An Analytical Technique Implemented in the Fractional Clannish Random Walker's Parabolic Equation with Nonlinear Physical Phenomena

Md. Nur Alam ¹, Imran Talib ², Omar Bazighifan ^{3,*}, Dimplekumar N. Chalishajar ^{4,*} and Barakah Almarri ⁵

¹ Department of Mathematics, Pabna University of Science & Technology, Pabna 6600, Bangladesh; nuralam.pstu23@gmail.com or nuralam23@pust.ac.bd

² Department of Mathematics and Statistics, Faculty of Science and Technology, Virtual University of Pakistan, Lahore 54000, Pakistan; imrantaalib@gmail.com or imrantalib@vu.edu.pk

³ Department of Mathematics, Faculty of Science, Hadhramout University, Hadhramout 50512, Yemen

⁴ Department of Applied Mathematics, Virginia Military Institute, 435 Mallory Hall, Letcher Av, Lexington, VA 24450, USA

⁵ Mathematical Science Department, Faculty of Science, Princess Nourah bint Abdulrahman University, Riyadh 11564, Saudi Arabia; BAlmarri@pnu.edu.sa

* Correspondence: o.bazighifan@gmail.com (O.B.); chalishajardn@vmi.edu (D.N.C.)

Abstract: In this paper, the adapted (G'/G) -expansion scheme is executed to obtain exact solutions to the fractional Clannish Random Walker's Parabolic (FCRWP) equation. Some innovative results of the FCRWP equation are gained via the scheme. A diverse variety of exact outcomes are obtained. The proposed procedure could also be used to acquire exact solutions for other nonlinear fractional mathematical models (NLFMMs).

Keywords: FCRWP; adapted (G'/G) -expansion scheme; exact solutions; fractional calculus; nonlinear dynamics



Citation: Alam, M.N.; Talib, I.; Bazighifan, O.; Chalishajar, D.N.; Almarri, B. An Analytical Technique Implemented in the Fractional Clannish Random Walker's Parabolic Equation with Nonlinear Physical Phenomena. *Mathematics* **2021**, *9*, 801. <https://doi.org/10.3390/math9080801>

Academic Editor: António Mendes Lopes

Received: 1 March 2021

Accepted: 31 March 2021

Published: 7 April 2021

Publisher's Note: MDPI stays neutral with regard to jurisdictional claims in published maps and institutional affiliations.



Copyright: © 2021 by the authors. Licensee MDPI, Basel, Switzerland. This article is an open access article distributed under the terms and conditions of the Creative Commons Attribution (CC BY) license (<https://creativecommons.org/licenses/by/4.0/>).

1. Introduction

Nonlinear fractional mathematical models (NLFMMs) are widely employed to describe many substantial phenomena and fractional nonlinear dynamic applications in plasma physics, mathematics, nonlinear control theory, physics, stochastic dynamical systems, engineering, signal processing, image processing, electromagnetics, transport systems, communications, acoustics, genetic algorithms, and viscoelasticity, amongst others. To define the exact answers to NLFMMs, many dominant and well-organized systems have been constructed and popularized, such as the variation of the (G'/G) -expansion scheme [1], adapted (G'/G) -expansion technique [2–5], exponential ansatz method [6], fractional iteration algorithm [7,8], the unified method [9], the first integral technique [10], the subequation scheme [11], improved fractional subequation scheme [12], the Jacobi elliptic ansatz method [13], generalized Kudryashov technique [14,15], novel extended direct algebraic method [16], natural transform method [17], fractional sub-equation scheme [18], exp-task scheme [19], generalized exponential rational task scheme [20], Kudryashov technique [21], sine-Gordon expansion technique [22], and the Jacobi elliptic task scheme [23]. Ma et al. [24] recently discovered a profoundly significant enlargement of the (G'/G) -extension process, called the adapted (G'/G) -expansion process, to secure exact solutions to NLFMMs. We used the adapted (G'/G) -expansion scheme for providing exact answers to the fractional Clannish Random Walker's Parabolic (FCRWP) equation in an ongoing effort to express it using a suitable and simple process. Therefore, we effortlessly exchange the FCRWP equation into a nonlinear partial differential equation (NPDE) or nonlinear ordinary differential equation (NODE) via the appropriate conversion to facilitate the process for those acquainted with fractional calculus. The main advantage of the process

implemented in this study compared with the basic (G'/G) -extension scheme is that it contributes additional novel exact answers, including added independent parameters. The implemented process takes all the responses received by the basic (G'/G) -extension scheme as a particular event, and we generate a few novel results. The exact answers are significant for uncovering the fundamental devices of physical events. Apart from the dynamic relevance, the exact answers to NLFMMs support numerical solvers when comparing their results' accuracies and help them in the stability analysis.

The remainder of this paper is organized as follows: In Section 2, we present a few analyses of the adapted (G'/G) -expansion scheme. In Section 3, we obtain answers to the FCRWP equation via the suggested method. In Section 4, we present some numerical simulations of the obtained solutions. In the last section, we present our conclusions.

2. Glimpse of the Technique

First, we provide a few ideas from fractional calculus theory and then present our proposed technique. For an outline of fractional calculus, we refer the reader to Refs. [25–27]. Numerous distinct varieties of fractional derivative operators have been recognized, such as: Atangana–Baleanu derivative [28], the Mittag–Leffler matrix function [29], Caputo–Fabrizio [30], the fractional boundary value problem with Sturm–Liouville boundary conditions [31], the Caputo derivative [27], the fractional derivative [32], and the conformable derivative [33]. Now, we concisely analyze the modified Riemann–Liouville derivative (MRLD) from the current fractional calculus recommended by Jumarie [34,35]. This leads to our study technique. Let $S : [0, 1] \rightarrow \Re$ be a continuous function and $\beta \in (0, 1)$. The Jumarie-improved fractional derivative of order β and S might be well-defined by [36]

$$D_x^\beta S(x) = \begin{cases} \frac{1}{\Gamma(-\beta)} \int_0^x (x - \chi)^{-\beta-1} [S(\chi) - S(0)] d\chi, & 0 > \beta, \\ \frac{1}{\Gamma(1-\beta)} \frac{d}{dx} \int_0^x (x - \chi)^{-\beta} [S(\chi) - S(0)] d\chi, & 0 < \beta < 1, \\ (S^{(n)}(x))(\beta - n), & n \leq \beta \leq n + 1, n \geq 1. \end{cases} \tag{1}$$

In addition to this representation, we preliminarily describe some properties of the fractional MRLD, which are later implemented in this paper. A few of the convenient procedures are assumed as:

$$D_x^\beta A = 0 \text{ (} A \text{ is a constant)} \tag{2}$$

$$D_x^\beta x^B = \begin{cases} 0, & (B \leq \beta - 1), \\ \frac{\Gamma(B+1)}{\Gamma(B-\beta+1)} x^{B-\beta}, & (B > \beta - 1). \end{cases} \tag{3}$$

$$D_x^\beta (C_1 R(x) + C_2 S(x)) = C_1 D_x^\beta R(x) + C_2 D_x^\beta S(x), \text{ (} C_1 \text{ and } C_2 \text{ are constants)} \tag{4}$$

$$D_x^\beta (R(x)S(x)) = S(x)D_x^\beta R(x) + R(x)D_x^\beta S(x), \tag{5}$$

$$S(x) = \sum_{A=0}^\infty \binom{n}{A} R^{(A)}(x) D_x^{\beta-A} S(x),$$

$$D_x^\beta [T(S(x))] = T'_5(S) = D_x^\beta S(x) = D_x^\beta T(S)(S_x)^\beta, d^\beta x(t) = \Gamma(1 + \beta) dx(t). \tag{6}$$

We consider

$$P(\lambda, \lambda_x, \lambda_{xx}, \lambda_t, \lambda_{tt}, \lambda_{xt}, \dots) = 0, \tag{7}$$

where P is a polynomial in λ and its partial derivatives.

Firstly, use the travelling variable:

$$\lambda = \lambda(x, t) = \lambda(\chi), \chi = p_3(x - Vt), \tag{8}$$

where p_3 and V are constants to be determined later. Substituting Equation (8) into Equation (7), we obtain:

$$R(\lambda, p_3\lambda', p_3^2\lambda'', -p_3V\lambda', p_3^2V^2\lambda'', -p_3^2V^2\lambda'', \dots) = 0. \tag{9}$$

Firstly, considering the ansatz form:

$$\lambda(\chi) = \sum_{i=-M}^M S_i h^i \tag{10}$$

where $h = \left(\frac{G'}{G} + \frac{\lambda}{2}\right)$, $|S_{-M}| + |S_M| \neq 0$, and $G = G(\chi)$ satisfy the equation.

$$G'' + \lambda G' + \mu G = 0, \tag{11}$$

where $S_i (\pm 1, \pm 2, \dots, \pm M)$, and λ and μ are coefficient constants defined later. Implementing the homogeneous balance principle in Equation (9), the positive integer M can be determined. From Equation (11), we find that

$$\hbar' = r - \hbar^2, \tag{12}$$

where $r = \frac{\lambda^2 - 4\mu}{4}$, and r is calculated by λ and μ . So, \hbar satisfies Equation (12), which produces:

$$h = \begin{cases} \sqrt{r} \tanh(\sqrt{r}\chi), & r > 0; \\ \sqrt{r} \coth(\sqrt{r}\chi), & r > 0; \\ \frac{1}{\chi}, & r = 0; \\ -\sqrt{r} \tan(\sqrt{-r}\chi), & r < 0; \\ -\sqrt{r} \cot(\sqrt{-r}\chi), & r < 0. \end{cases} \tag{13}$$

Finally, by implementing Equations (9) and (10) and collecting all terms with the same order of \hbar together, the left-hand side of Equation (10) is converted into a polynomial in \hbar . Equating each coefficient of the polynomial to zero, we can obtain a set of algebraic equations that can be solved to find the values of the studied method.

3. Mathematical Analysis

In this paper, we consider the FCRWP equation [37]:

$$\frac{\partial^\beta \lambda}{\partial t^\beta} - \frac{\partial \lambda}{\partial x} + 2\lambda \frac{\partial \lambda}{\partial x} + \frac{\partial^2 \lambda}{\partial x^2} = 0, \quad t > 0, \quad 0 < \beta, \tag{14}$$

with $\lambda(x, 0) = S(x)$. Taking the variable transformation $\lambda(x, t) = \lambda(\chi)$, $\chi = x - \frac{Vt^\beta}{\Gamma(1+\beta)}$ in Equation (14), we have:

$$-V\lambda' - \lambda' + 2\lambda\lambda' - \lambda'' = 0. \tag{15}$$

The pole of Equation (15) is given as $N = 1$. Then, we find from Equation (10) that:

$$\lambda(\chi) = \sum_{i=-1}^1 S_i \hbar^i \tag{16}$$

Collecting the coefficient of Equation (14) and finding the resulting system, we then find:

$$\text{Group I: } V = 2S_0 - 1, S_1 = 0, S_{-1} = -\frac{1}{4}\lambda^2 + \mu. \tag{17}$$

Substituting the above values into Equation (15), we obtain:

$$\lambda_{11}(\chi) = S_0 + \left(-\frac{1}{4}\lambda^2 + \mu\right) \times \left\{ \frac{\sqrt{\lambda^2 - 4\mu}}{2} \tanh\left(\frac{\sqrt{\lambda^2 - 4\mu}}{2} \chi\right) \right\}^{-1}. \tag{18}$$

$$\lambda_{12}(\chi) = S_0 + (-\frac{1}{4}\lambda^2 + \mu) \times \left\{ \frac{\sqrt{\lambda^2 - 4\mu}}{2} \coth\left(\frac{\sqrt{\lambda^2 - 4\mu}}{2}\chi\right) \right\}^{-1} \tag{19}$$

$$\lambda_{13}(\chi) = S_0 + (-\frac{1}{4}\lambda^2 + \mu) \times \left(\frac{1}{\chi}\right)^{-1} \tag{20}$$

$$\lambda_{14}(\chi) = S_0 + (-\frac{1}{4}\lambda^2 + \mu) \times \left\{ -\frac{\sqrt{4\mu - \lambda^2}}{2} \tan\left(\frac{\sqrt{4\mu - \lambda^2}}{2}\chi\right) \right\}^{-1} \tag{21}$$

$$\lambda_{15}(\chi) = S_0 + (-\frac{1}{4}\lambda^2 + \mu) \times \left\{ -\frac{\sqrt{4\mu - \lambda^2}}{2} \cot\left(\frac{\sqrt{4\mu - \lambda^2}}{2}\chi\right) \right\}^{-1} \tag{22}$$

$$\text{Group II : } V = 2S_0 - 1, S_1 = -1, S_{-1} = 0. \tag{23}$$

Similarly, we obtain:

$$\lambda_{21}(\chi) = S_0 - \left\{ \frac{\sqrt{\lambda^2 - 4\mu}}{2} \tanh\left(\frac{\sqrt{\lambda^2 - 4\mu}}{2}\chi\right) \right\}. \tag{24}$$

$$\lambda_{22}(\chi) = S_0 - \left\{ \frac{\sqrt{\lambda^2 - 4\mu}}{2} \coth\left(\frac{\sqrt{\lambda^2 - 4\mu}}{2}\chi\right) \right\}. \tag{25}$$

$$\lambda_{23}(\chi) = S_0 - \left(\frac{1}{\chi}\right). \tag{26}$$

$$\lambda_{24}(\chi) = S_0 - \left\{ -\frac{\sqrt{4\mu - \lambda^2}}{2} \tan\left(\frac{\sqrt{4\mu - \lambda^2}}{2}\chi\right) \right\}. \tag{27}$$

$$\lambda_{25}(\chi) = S_0 - \left\{ -\frac{\sqrt{4\mu - \lambda^2}}{2} \cot\left(\frac{\sqrt{4\mu - \lambda^2}}{2}\chi\right) \right\}. \tag{28}$$

$$\text{Group III : } V = 2S_0 - 1, S_1 = -1, S_{-1} = -\frac{1}{4}\lambda^2 + \mu. \tag{29}$$

Similarly, we obtain:

$$\begin{aligned} \lambda_{31}(\chi) = & S_0 - \left\{ \frac{\sqrt{\lambda^2 - 4\mu}}{2} \tanh\left(\frac{\sqrt{\lambda^2 - 4\mu}}{2}\chi\right) \right\} \\ & + (-\frac{1}{4}\lambda^2 + \mu) \times \left\{ \frac{\sqrt{\lambda^2 - 4\mu}}{2} \tanh\left(\frac{\sqrt{\lambda^2 - 4\mu}}{2}\chi\right) \right\}^{-1} \end{aligned} \tag{30}$$

$$\begin{aligned} \lambda_{32}(\chi) = & S_0 - \left\{ \frac{\sqrt{\lambda^2 - 4\mu}}{2} \coth\left(\frac{\sqrt{\lambda^2 - 4\mu}}{2}\chi\right) \right\} \\ & + (-\frac{1}{4}\lambda^2 + \mu) \times \left\{ \frac{\sqrt{\lambda^2 - 4\mu}}{2} \coth\left(\frac{\sqrt{\lambda^2 - 4\mu}}{2}\chi\right) \right\}^{-1} \end{aligned} \tag{31}$$

$$\lambda_{33}(\chi) = S_0 - \left(\frac{1}{\chi}\right) + (-\frac{1}{4}\lambda^2 + \mu) \times \left(\frac{1}{\chi}\right)^{-1} \tag{32}$$

$$\begin{aligned} \lambda_{34}(\chi) = & S_0 - \left\{ -\frac{\sqrt{4\mu - \lambda^2}}{2} \tan\left(\frac{\sqrt{4\mu - \lambda^2}}{2}\chi\right) \right\} \\ & + (-\frac{1}{4}\lambda^2 + \mu) \times \left\{ -\frac{\sqrt{4\mu - \lambda^2}}{2} \tan\left(\frac{\sqrt{4\mu - \lambda^2}}{2}\chi\right) \right\}^{-1} \end{aligned} \tag{33}$$

$$\begin{aligned} \lambda_{35}(\chi) = & S_0 - \left\{ -\frac{\sqrt{4\mu - \lambda^2}}{2} \cot\left(\frac{\sqrt{4\mu - \lambda^2}}{2}\chi\right) \right\} \\ & + (-\frac{1}{4}\lambda^2 + \mu) \times \left\{ -\frac{\sqrt{4\mu - \lambda^2}}{2} \cot\left(\frac{\sqrt{4\mu - \lambda^2}}{2}\chi\right) \right\}^{-1} \end{aligned} \tag{34}$$

4. Numerical Simulations

Ma et al. [24] introduced a process named the revised (G'/G)-extension approach to look for the FCRWP equation's exact structures and achieved fifteen results, shown in Section 3. Gunner et al. [37] reported a process named the (G'/G)-extension approach to look for the FCRWP equation's exact structures and achieved three results. In comparing the two methods, the revised (G'/G)-extension approach provides a more exact answer than the (G'/G)-extension approach. In terms of additional support, the auxiliary model

employed in the integral method is different, so the exact structures obtained are also different. Likewise, for any NLFMM, it could be determined that the revised (G'/G)-extension approach is much more straightforward than the other schemes. In this paper, the integrable method is applied to the FCRWP equation for the first time. We confirm that no other author has used the technique on the FCRWP equation. This paper expresses various varieties of exact solutions of the answers for countless values of the constant coefficients. The exact solutions are: dark soliton profiles, singular kink profiles, dark singular soliton profiles, bright and dark lump shapes, periodic wave profiles, etc. Furthermore, we offer a contour graph of the obtained answers, which was created by commencing binary variable tasks. One variable is demonstrated on the horizontal and vertical axes of the contour graph. The functional value exemplifies the color gradient and isolines. The contour graph is a technique used to express a 3D surface on a 2D plane. This kind of graph is broadly implemented in mathematics, physics, as well as engineering, where the contour lines normally represent elevation. We obtained exact solutions like trigonometric, hyperbolic, and rational function answers through the proposed procedure. The solutions to $\lambda_{11}(\chi)$, $\lambda_{12}(\chi)$, $\lambda_{21}(\chi)$, $\lambda_{22}(\chi)$, $\lambda_{31}(\chi)$, and $\lambda_{32}(\chi)$ present as trigonometric function solutions; the solutions of $\lambda_{14}(\chi)$, $\lambda_{15}(\chi)$, $\lambda_{24}(\chi)$, $\lambda_{25}(\chi)$, $\lambda_{34}(\chi)$, and $\lambda_{35}(\chi)$ present as hyperbolic function solutions; and the solutions of $\lambda_{13}(\chi)$, $\lambda_{23}(\chi)$, and $\lambda_{33}(\chi)$ present as trigonometric function solutions. We explain the dynamic performance of the trigonometric function answers of $\lambda_{11}(\chi)$, $\lambda_{12}(\chi)$, $\lambda_{22}(\chi)$, and $\lambda_{31}(\chi)$, which are illustrated in Figures 1–4. In particular, Figures 1–4 demonstrate the 3D shape, contour plot, and 2D graph for different values of α for the trigonometric function answers of $\lambda_{11}(\chi)$, $\lambda_{12}(\chi)$, $\lambda_{22}(\chi)$, and $\lambda_{31}(\chi)$. We explain the dynamic performance of the rational function answers to $\lambda_{23}(\chi)$ and $\lambda_{33}(\chi)$, as illustrated in Figures 5 and 6. Figures 5 and 6 demonstrate the 3D shape, contour plot, and 2D graph for different values of α for the rational function answers to $\lambda_{23}(\chi)$ and $\lambda_{33}(\chi)$. Finally, we explain the dynamic performance of the trigonometric function answers of $\lambda_{14}(\chi)$, $\lambda_{15}(\chi)$, $\lambda_{25}(\chi)$, and $\lambda_{34}(\chi)$ in Figures 7–10, which depict the 3D shape, contour plot, and 2D graph for different values of α for the trigonometric function answers of $\lambda_{14}(\chi)$, $\lambda_{15}(\chi)$, $\lambda_{25}(\chi)$, and $\lambda_{34}(\chi)$. The implemented mathematical simulations acknowledge that the answers are of periodic wave shapes and of rational, hyperbolic, and trigonometric categorizations. Furthermore, through observing the construction of the acquired answers, it could be understood that the connecting fractional derivatives of parameter α perform in the formulation of all the answers.

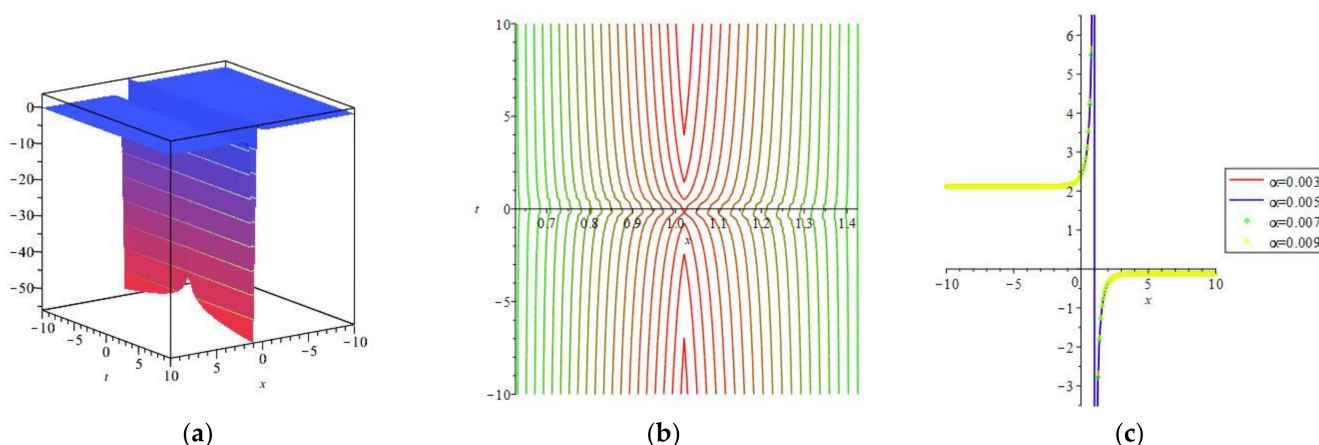


Figure 1. The graphical representation of the solution $\lambda_{11}(\chi)$: (a) 3D shape, (b) contour plot, and (c) 2D graph.

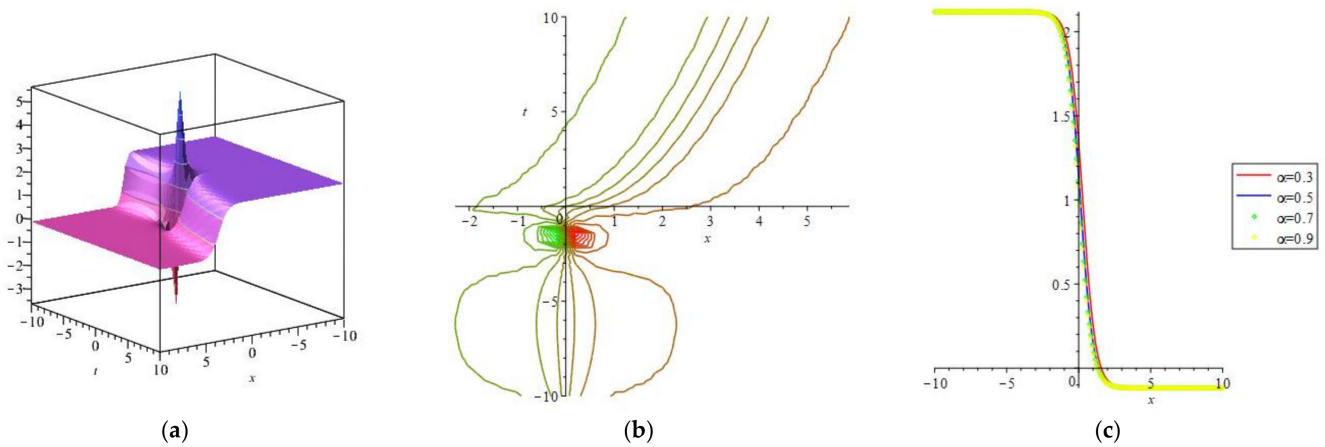


Figure 2. The graphical representation of the solution $\lambda_{12}(\chi)$: (a) 3D shape, (b) contour plot, and (c) 2D graph.

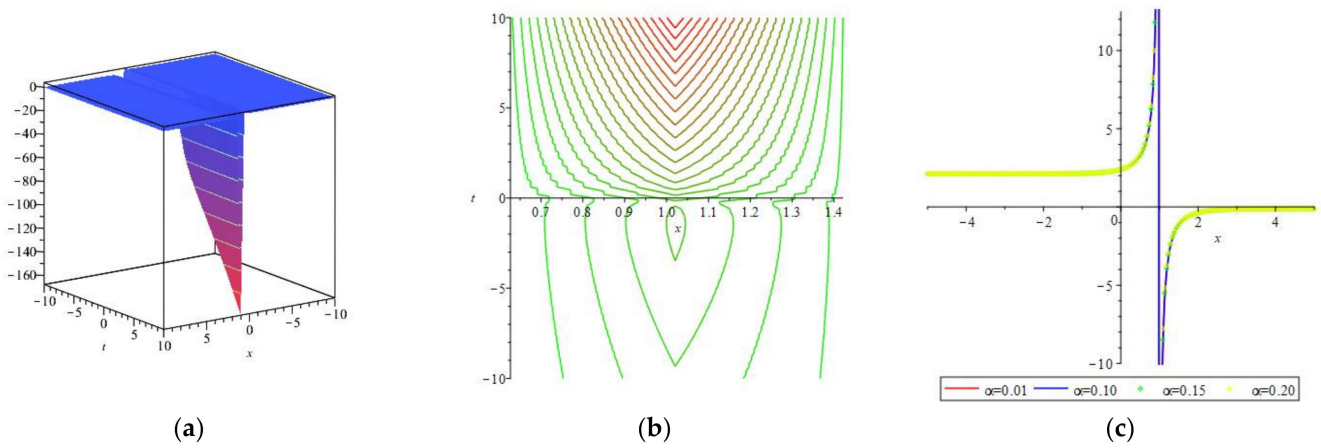


Figure 3. The graphical representation of the solution $\lambda_{22}(\chi)$: (a) 3D shape, (b) contour plot, and (c) 2D graph.

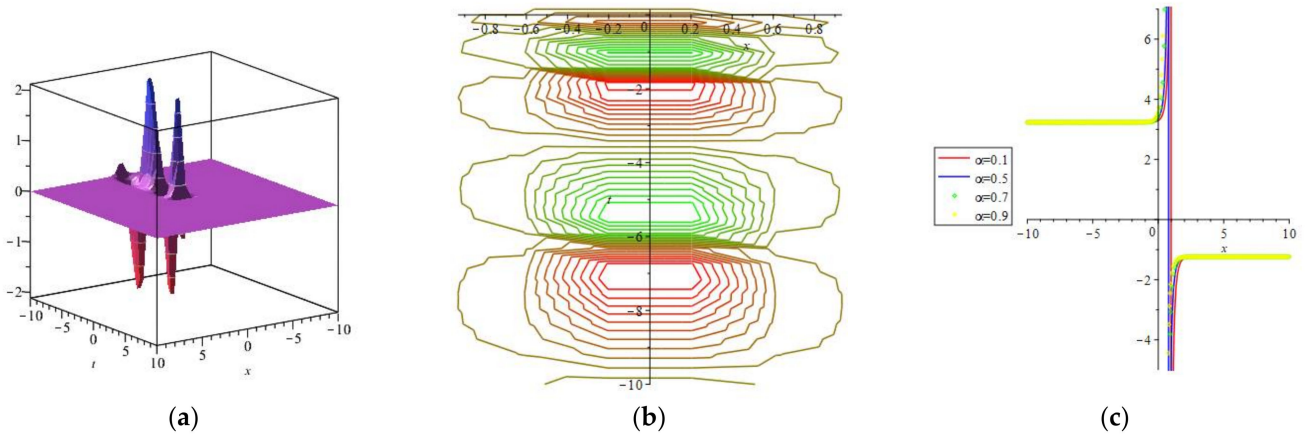


Figure 4. The graphical representation of the solution $\lambda_{31}(\chi)$: (a) 3D shape, (b) contour plot, and (c) 2D graph.

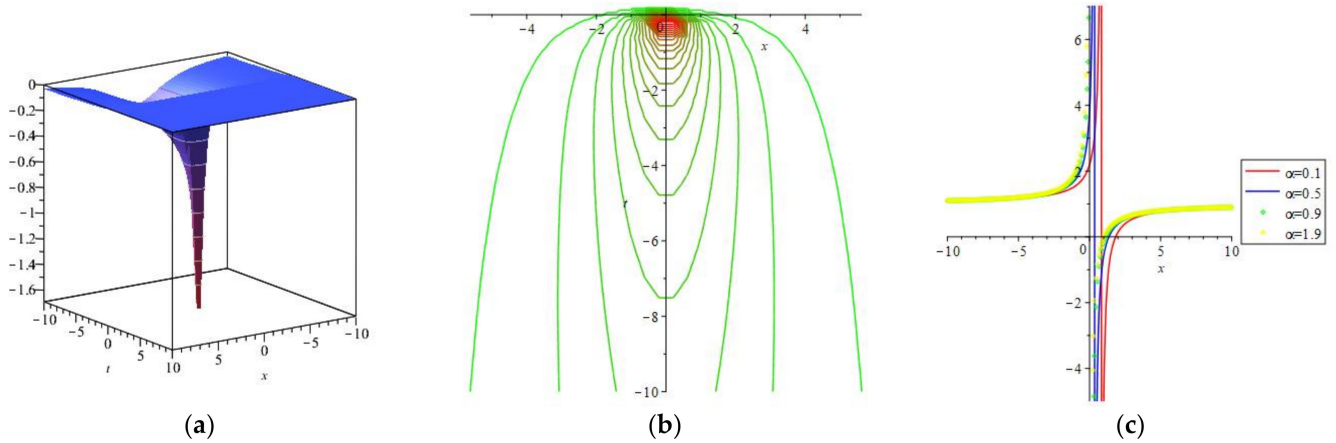


Figure 5. The graphical representation of the solution $\lambda_{23}(\chi)$: (a) 3D shape, (b) contour plot, and (c) 2D graph.

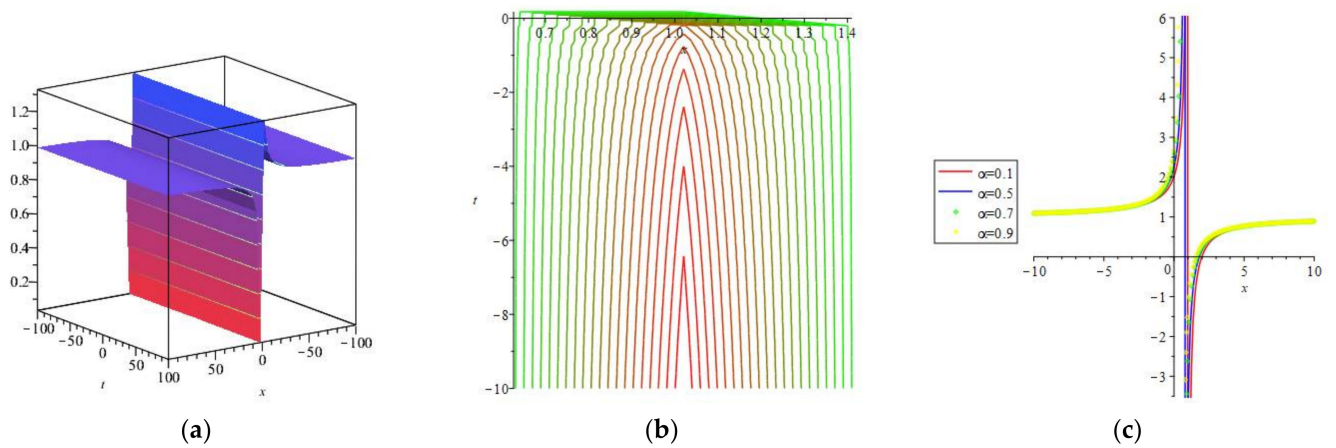


Figure 6. The graphical representation of the solution $\lambda_{33}(\chi)$: (a) 3D shape, (b) contour plot, and (c) 2D graph.

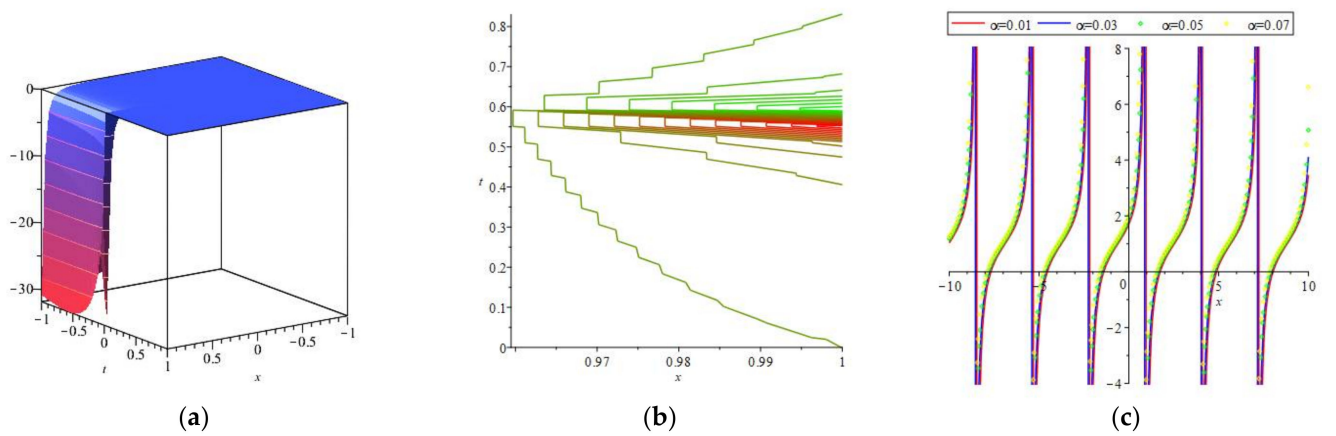


Figure 7. The graphical representation of the solution $\lambda_{14}(\chi)$: (a) 3D shape, (b) contour plot, and (c) 2D graph

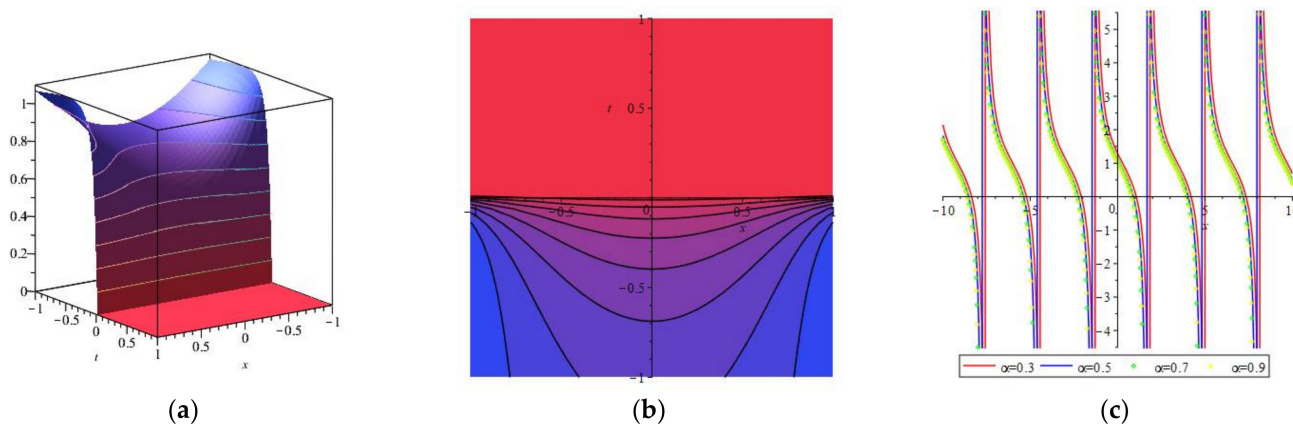


Figure 8. The graphical representation of the solution $\lambda_{15}(\chi)$: (a) 3D shape, (b) contour plot, and (c) 2D graph.

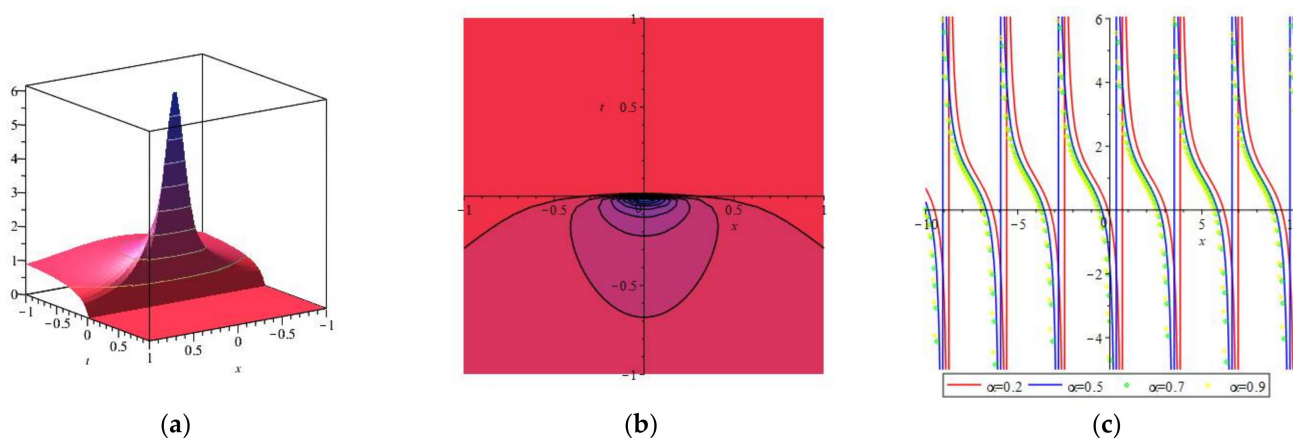


Figure 9. The graphical representation of the solution $\lambda_{25}(\chi)$: (a) 3D shape, (b) contour plot, and (c) 2D graph.

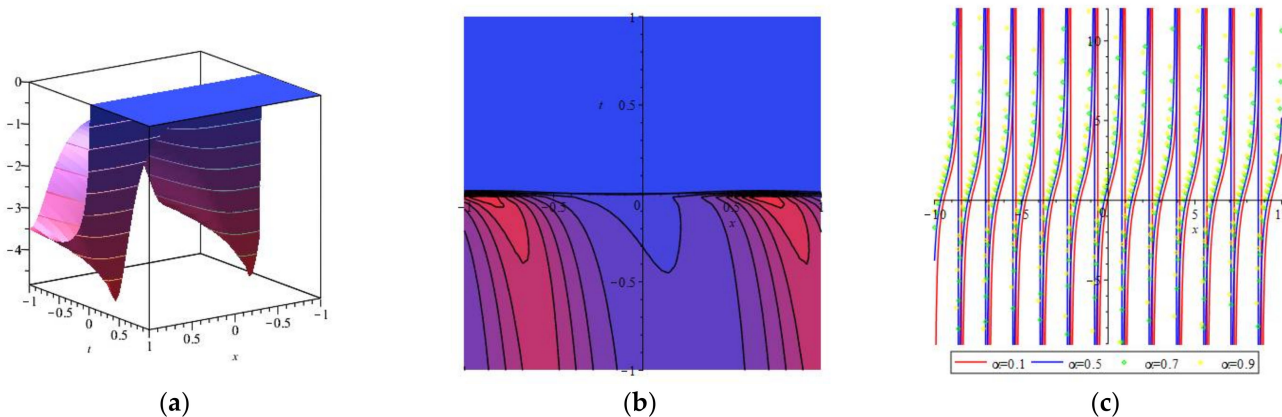


Figure 10. The graphical representation of the solution $\lambda_{34}(\chi)$: (a) 3D shape, (b) contour plot, and (c) 2D graph.

5. Conclusions

In this investigation, we successfully devised a procedure that demonstrates that this system is well-organized and effectively acceptable for finding the exact answers to the FCRWP equation. A wide variety of dynamical behaviors were considered in this study, which presented in well-defined regions of mathematical physics. The most important advantage of this method is that it can more easily reach the solutions than the other analytical schemes for solving NLFMMs. These answers will be valuable for further studies in mathematical physics.

Author Contributions: Conceptualization, M.N.A., I.T., O.B., D.N.C. and B.A. All authors have read and agreed to the published version of the manuscript.

Funding: This research was funded by the Deanship of Scientific Research at Princess Nourah bint Abdulrahman University through the Fast-track Research Funding Program.

Institutional Review Board Statement: Not applicable.

Informed Consent Statement: Not applicable.

Data Availability Statement: Not applicable.

Acknowledgments: The authors thank the reviewers for their useful comments, which led to the improvement of the content of the paper. The authors would like to thank the Deanship of Scientific Research at Princess Nourah Bint Abdulrahman University for funding this work through the Fast-track Research Funding Program.

Conflicts of Interest: The authors declare no conflict of interest.

References

1. Alam, M.N.; Seadawy, A.R.; Baleanu, D. Closed-form wave structures of the space-timefractional Hirota–Satsuma coupled KdV equation with nonlinear physical phenomena. *Open Phys.* **2021**, *18*, 555–565. [[CrossRef](#)]
2. Islam, S.; Alam, M.N.; Asad, M.F.A.; Tunc, C. An analytical technique for solving new computational solutions of the modified Zakharov–Kuznetsov equation arising in electrical engineering. *J. Appl. Comput. Mech.* **2021**, *7*, 715–726.
3. Alam, M.N.; Tunc, C. The new solitary wave structures for the $(2 + 1)$ -dimensional time-fractional Schrödinger equation and the space-time nonlinear conformable fractional Bogoyavlenskii equations. *Alex. Eng. J.* **2020**, *59*, 2221–2232. [[CrossRef](#)]
4. Alam, M.N.; Li, X. New soliton solutions to the nonlinear complex fractional Schrödinger equation and the conformable time-fractional Klein–Gordon equation with quadratic and cubic nonlinearity. *Phys. Scr.* **2020**, *95*, 045224. [[CrossRef](#)]
5. Alam, M.N.; Osman, M.S. New structures for closed-form wave solutions for the dynamical equations model related to the ion sound and Langmuir waves. *Commun. Theor. Phys.* **2021**, *73*, 035001. [[CrossRef](#)]
6. Park, C.; Nuruddeen, R.I.; Ali, K.K.; Muhammad, L.; Osman, M.S.; Baleanu, D. Novel hyperbolic and exponential ansatz methods to the fractional fifth-order Korteweg–de Vries equations. *Adv. Differ. Equ.* **2020**, *2020*, 627. [[CrossRef](#)]
7. Ahmad, H.; Khan, T.A.; Ahmad, I.; Stanimirović, P.S.; Chu, Y.M. A new analyzing technique for nonlinear time fractional Cauchy reaction–diffusion model equations. *Results Phys.* **2020**, *19*, 103462. [[CrossRef](#)]
8. Ahmad, H.; Akgül, A.; Khan, T.A.; Stanimirović, P.S.; Chu, Y.M. New perspective on the conventional solutions of the nonlinear time fractional partial differential equations. *Complexity* **2020**, *2020*, 8829017. [[CrossRef](#)]
9. Osman, M.S.; Rezazadeh, H.; Eslami, M. Traveling wave solutions for $(3 + 1)$ dimensional conformable fractional Zakharov–Kuznetsov equation with power law nonlinearity. *Nonlinear Eng.* **2019**, *8*, 559–567. [[CrossRef](#)]
10. Yeppez-Martinez, H.; Gomez-Aguilar, J.F.; Atangana, A. First integral method for non-linear differential equations with conformable derivative. *Math. Model. Nat. Phenom.* **2018**, *13*, 14. [[CrossRef](#)]
11. Aminikhah, H.; Sheikhan, A.H.R.; Rezazadeh, H. Sub-equation method for the fractional regularized long-wave equations with conformable fractional derivatives. *Sci. Iran.* **2016**, *23*, 1048–1054. [[CrossRef](#)]
12. Jiang, J.; Feng, Y.; Li, S. Improved fractional sub-equation method and exact solutions to fractional partial differential equations. *J. Funct. Sp.* **2020**, *2020*, 5840920.
13. Aslan, E.C.; Inc, M. Optical soliton solutions of the NLSE with quadratic-cubic-hamiltonian perturbations and modulation instability analysis. *Optik* **2019**, *196*, 162661. [[CrossRef](#)]
14. Gurefe, Y. The generalized Kudryashov method for the nonlinear fractional partial differential equations with the beta-derivative. *Rev. Mex. Física* **2020**, *66*, 771–781. [[CrossRef](#)]
15. Alam, M.N.; Bonyah, E.; Asad, M.F.A.; Osman, M.S.; Abualnaja, K.M. Stable and functional solutions of the Klein–Fock–Gordon equation with nonlinear physical phenomena. *Phys. Scr.* **2021**. accepted. [[CrossRef](#)]
16. Tozar, A.; Kurt, A.; Tasbozan, O. New wave solutions of time fractional integrable dispersive wave equation arising in ocean engineering models. *Kuwait J. Sci.* **2020**, *47*, 22–33.
17. Ismail, G.M.; Rahim, H.R.A.; Aty, A.A.; Kharabsheh, R.; Alharbi, W.; Aty, M.A. An analytical solution for fractional oscillator in a resisting medium. *Chaos Solitons Fract.* **2020**, *130*, 109395. [[CrossRef](#)]
18. Yeppez-Martinez, H.; Gomez-Aguilar, J.F. Fractional sub-equation method for Hirota–Satsuma-coupled KdV equation and coupled mKdV equation using the Atangana’s conformable derivative. *Waves Random Complex Media* **2019**, *29*, 678–693. [[CrossRef](#)]
19. Hosseini, K.; Mirzazadeh, M.; Rabiei, F.; Baskonus, H.M.; Yel, G. Dark optical solitons to the Biswas–Arshed equation with high order dispersions and absence of the self-phase modulation. *Optik* **2020**, *209*, 164576. [[CrossRef](#)]
20. Ghanbari, B.; Baleanu, D. New Optical Solutions of the Fractional Gerdjikov–Ivanov Equation with Conformable Derivative. *Front. Phys.* **2020**, *8*, 167. [[CrossRef](#)]
21. Hosseini, K.; Mirzazadeh, M.; Ilie, M.; Radmehr, S. Dynamics of optical solitons in the perturbed Gerdjikov–Ivanov equation. *Optik* **2020**, *206*, 164350. [[CrossRef](#)]

22. Korkmaz, A.; Hepson, O.E.; Hosseini, K.; Rezazadeh, H.; Eslami, M. Sine-gordon expansion method for exact solutions to conformable time fractional equations in RLW-class. *J. King Saud Univ. Sci.* **2020**, *32*, 567–574. [[CrossRef](#)]
23. Hosseini, K.; Mirzazadeh, M.; Vahidi, J.; Asghari, R. Optical wave structures to the Fokas–Lenells equation. *Optik* **2020**, *207*, 164450. [[CrossRef](#)]
24. Ma, X.; Pan, Y.; Chang, L. The modified (G'/G) -expansion method and its applications to KdV equation. *Int. J. Nonlinear Sci.* **2011**, *12*, 400–404.
25. Miller, K.S.; Ross, B. *An Introduction to the Fractional Calculus and Fractional Differential Equations*; Wiley: New York, NY, USA, 1993.
26. Kilbas, A.A.; Srivastava, H.M.; Trujillo, J.J. *Theory and Applications of Fractional Differential Equations*; Elsevier: San Diego, CA, USA, 2006.
27. Podlubny, I. *Fractional Differential Equations*; Academic Press: Cambridge, MA, USA, 1999.
28. Atangana, A.; Baleanu, D. New fractional derivatives with nonlocal and non-singular kernel: Theory and application to heat transfer model. *Therm. Sci.* **2016**, *20*, 763–769. [[CrossRef](#)]
29. Kumar, A.; Vats, R.K.; Kumar, A.; Chalisahaj, D.N. Numerical approach to the controllability of fractional order impulsive differential equations. *Demonstr. Math.* **2020**, *53*, 193–207. [[CrossRef](#)]
30. Caputo, M.; Fabrizio, M. A new definition of fractional derivative without singular kernel. *Progr. Fract. Differ. Appl.* **2015**, *1*, 73–85. [[CrossRef](#)]
31. Harjani, J.; López, B.; Sadarangani, K. Existence and uniqueness of mild solutions for a fractional differential equation under Sturm-Liouville boundary conditions when the data function is of Lipschitzian type. *Demonstr. Math.* **2020**, *53*, 167–173. [[CrossRef](#)]
32. Khalil, R.; Horani, M.A.; Yousef, A.; Sababheh, M. A new definition of fractional derivative. *J. Comput. Appl. Math.* **2014**, *264*, 65–70. [[CrossRef](#)]
33. Atangana, A.; Baleanu, D.; Alsaedi, A. New properties of conformable derivative. *Open Math.* **2015**, *13*, 889–898. [[CrossRef](#)]
34. Jumarie, G. Modified Riemann-Liouville derivative and fractional Taylor series of nondifferentiable functions further results. *Comput. Math. Appl.* **2006**, *51*, 1367–1376. [[CrossRef](#)]
35. Jumarie, G. Table of some basic fractional calculus formulae derived from a modified Riemann-Liouville derivative for non-differentiable functions. *Appl. Math. Lett.* **2009**, *22*, 378–385. [[CrossRef](#)]
36. Ganji, Z.; Ganji, D.; Ganji, A.D.; Rostamian, M. Analytical solution of time-fractional Navier–Stokes equation in polar coordinate by homotopy perturbation method. *Numer. Methods Partial Differ. Equ.* **2010**, *26*, 117–124. [[CrossRef](#)]
37. Gunera, O.; Bekir, A.; Ünsal, Ö. Two reliable methods for solving the time fractional Clannish Random Walker’s Parabolic equation. *Optik* **2016**, *127*, 9571–9577. [[CrossRef](#)]